ACS OMEGA

http://pubs.acs.org/journal/acsodf

Article

Conserved Apical Proline Regulating the Structure and DNA Binding Properties of *Helicobacter pylori* Histone-like DNA Binding Protein (Hup)

Nipanshu Agarwal, Nupur Nagar, Ritu Raj, Dinesh Kumar, and Krishna Mohan Poluri*

Cite This: *ACS Omega* 2022, 7, 15231−15246

Read Online

ACCESS | Metrics & More | Article Recommendations | Supporting Information

ABSTRACT: Prokaryotic cells lack a proper dedicated nuclear arrangement machinery. A set of proteins known as nucleoid associated proteins (NAPs) perform opening and closure of nucleic acids, behest cellular requirement. Among these, a special class of proteins analogous to eukaryotic histones popularly known as histone-like (HU) DNA binding proteins facilitate the nucleic acid folding/compaction thereby regulating gene architecture and gene regulation. DNA compaction and DNA protection in *Helicobacter pylori* is performed by HU protein (Hup). To dissect and galvanize the role of proline residue in the binding of Hup with DNA, the structure-dynamics-functional relationship of Hup-P64A variant was analyzed. NMR and biophysical studies evidenced that Hup-P64A protein attenuated DNA-binding and induced structural/stability changes in the DNA binding domain (DBD). Moreover, molecular dynamics simulations and ^{15}N relaxation studies established the reduced conformational dynamics of P64A protein. This comprehensive study dissected the exclusive role of evolutionarily conserved apical proline residue in regulating the structure and DNA binding of Hup protein as P64 is presumed to be involved in the external leverage mechanism responsible for DNA bending and packaging, as proline rings wedge into the DNA backbone through intercalation besides their significant role in DNA binding.

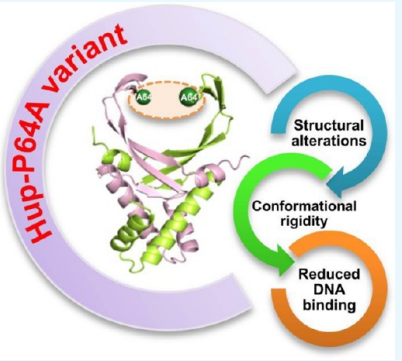

INTRODUCTION

In a cell, nucleic acid must arrange and organize into a compact structure to optimally accommodate all other cellular organelles in the limited/available space.[1,2] The DNA related processes such as DNA compaction, repair, recombination, transposition, replication, transcription, remodeling, and gene regulation require both regular access to nucleic acid and DNA binding.[1,3,4] Hence, nucleic acid organization is regularly managed by a class of nuclear architectural proteins that are collectively classified as nucleoid associated proteins (NAPs). In prokaryotes, out of several NAPs, a particular subset of proteins known as histone-like (HU) DNA binding proteins assists in DNA compaction, organization, and protection.[5,6] HU proteins possess several structural features that enable preferential DNA binding in cellular milieu. Atypically, the primary chain of amino acids in HU homologues fold to yield a monomer with three α-helices and four/five β-strands (Figure 1A).[7,8] Two monomer units self-associate and intertwine forming a dimeric structure which can be differentiated as homo-/heterodimers based on slight differences in participating subunits (Figure 1B). Each monomeric unit follows basic HU/IHF (integrative host factor) clade structural fold with α_1 and α_2 separated by a small loop region; β-strands ($\beta1-\beta5$) arranged in tandem between α_2 and α_3.[9,10] However, exceptional cases where a β-strand is present prior to α_1 helix, results in increased number of β-strands as observed in an HU homologue.[8] The dimeric structure thus formed has two functional domains i.e., dimerization domain (DD) and DNA binding domain (DBD) with their exclusive functions[7,11] (Figure 1B).

Dimerization domain (DD) acts as the foundation of the protein structure wherein hydrophobic interactions, electrostatic interactions and salt bridges maintain helix−turn−helix (HTH) topology.[12−16] On the other hand, the DBD is responsible for conferring functional relevance to the HU protein by binding to the DNA. HU proteins have several features that aid the binding of HU protein with DNA. To begin with, the basal floor of saddle shaped DBD has β-strands arranged in an antiparallel sequence. The residues in these β-strands are strategically placed to avoid N−H and C═O bonds, thus inhibiting formation of canonical β-sheets with utmost flexibility.[7,17] Through the base of saddle pocket emerges a β-arm structure that is modeled precisely to accommodate DNA binding by forming helical depression complementary to DNA topology (with ∼25 Å diameter)[7]

Received: March 23, 2022
Accepted: April 6, 2022
Published: April 18, 2022

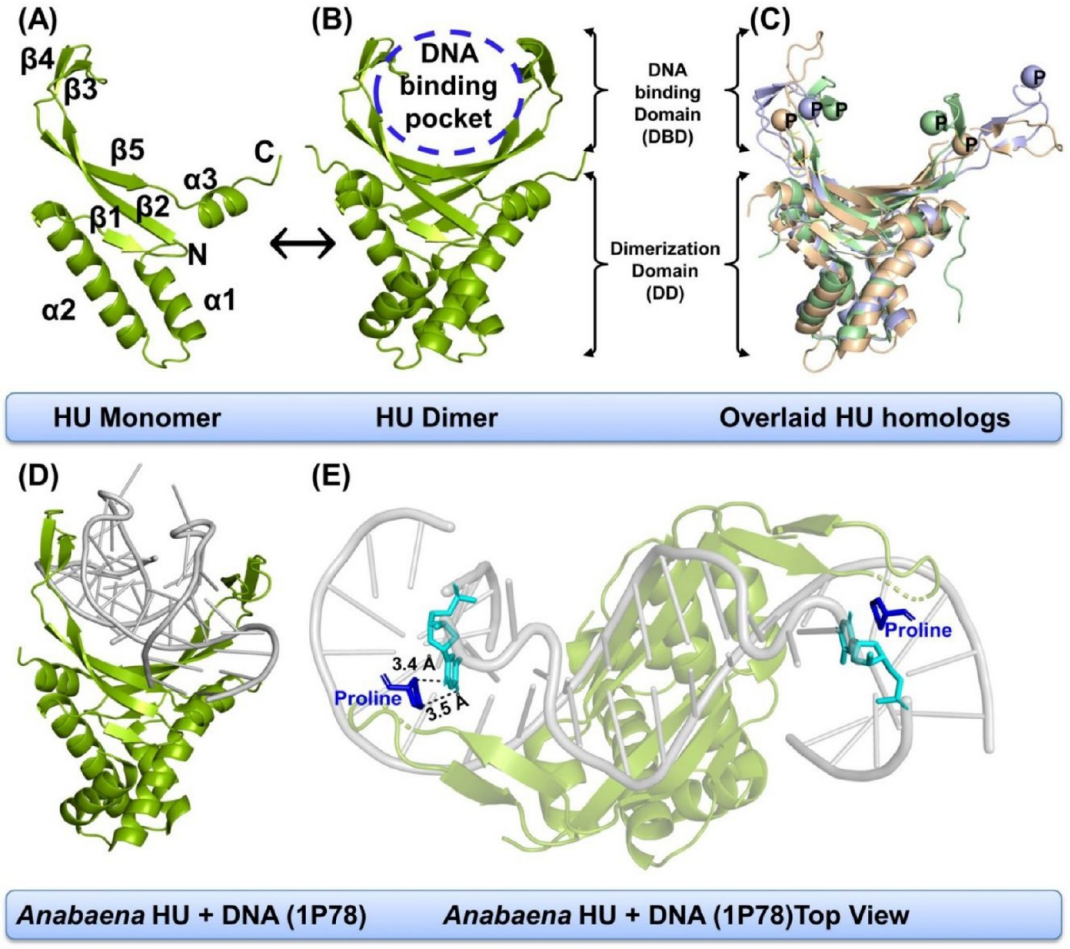

Figure 1. Structural features of HU family proteins. (A) Monomeric subunit showing secondary structural elements; Initial two α-helices (α1, and α2) and α3 helix at end interspersed with β1-β5 strands. (B) Dimeric conformation of HU protein comprising of DNA binding pocket, DNA binding domain (DBD) and Dimerization domain (DD). (C) Overlaid structure of HU homologues from *Mycobacterium tuberculosis* (green, PDB ID: 4PT4), *Mycoplasma gallisepticum* (peach, PDB ID: 2NDP), and *Geobacillus stearothermophilus* (purple, PDB ID: 1HUE) with their conserved apical proline residue represented as sphere of respective color. Structure of HU protein of *Anabaena* bound to DNA (PDB ID: 1P78): (D) lateral view and (E) top view showing interaction/intercalation of proline residues. The graphical structures were generated using PYMOL software.

(Figure 1B,C). Second, abundant placement of positively charged amino acids (arginine and lysine) provides an electrostatic milieu favorable for negatively charged DNA binding.[16,18]

In addition to that, HU proteins have a conserved proline residue that occupies apical position at β-arm facilitating intercalation of imino/pyrrolidine ring in between adjacent nucleotide base pairs of DNA[17,19,20] (Figure 1D,E). Evidence related to the involvement of this proline residue in DNA binding predates to the late 1980s or early 1990s, wherein phage complementation method was used to restore the loss of function mutation in *Escherichia coli* HU protein.[21] Although such loss of function has been accepted, correlated, and extrapolated to other sub categories of type-II DNA binding proteins belonging to the HU/IHF clade, yet no structural data highlighting molecular interactions of this evolutionarily conserved proline is reported.[19,20] Henceforth, investigations pertaining to the structural stability/DNA binding features of proline mutants from various members of HU family proteins are quintessential to comprehensively establish its unique role in the structure−stability−function relationship.

Like several prokaryotes, *Helicobacter pylori* also possess a HU homologue, denoted as Hup protein that shares 37% similarity with the consensus HU protein sequence and adapts the ancient DNABII structural fold.[22] Hup protein is involved in diverse cellular pathways like acid stress response, DNA related functions (compaction, protection, replication), immunological defense, and modulation of gene expression in *H. pylori*.[23−29] Recent studies on pH-dependent structure and DNA binding features of Hup protein unravelled its conformational heterogeneity, enhanced structural stability and equipotent DNA binding ability, thus establishing a significant role of Hup in the acid stress mitigation.[14] Therefore, in this current study, the evolutionarily conserved proline residue (P64, in Hup sequence) was modified to alanine (Hup-P64A protein) to analyze its regulatory role in structural stability and DNA binding of Hup protein. The study embodies the elucidation of the attenuated DNA binding ability of the P64A variant and modulation of structural preferences and molecular stability, thus highlighting its prime role in the structure−function relationship of the HU protein family.

MATERIALS AND METHODS

Site-Directed Mutagenesis, Protein Expression, and Purification. Site-directed mutagenesis method was used to generate the P64A mutant. Oligonucleotide primers with a

https://doi.org/10.1021/acsomega.2c01754
ACS Omega 2022, 7, 15231−15246

sequence as described in Table S1 were annealed at 53 °C in the polymerase chain reaction (PCR) reaction. The PCR product thus obtained was treated with Dpn I enzyme and later used to transform *E. coli* BL21 cells. Colonies observed on plates after overnight incubation were inoculated in Luria−Bertani (LB) broth, and the culture was used to extract plasmids. The correctness of the mutation was confirmed by DNA sequencing. Both the proteins (WT and P64A) were produced by overexpression at 16 °C using isopropyl β-D-1-thiogalactopyaranose (IPTG, 0.2 mM) as inducer. The proteins were expressed and purified using Ni^{2+} ion affinity chromatography as per the protocol described elsewhere.[14,30] Final buffer conditions for all the protein samples were 50 mM sodium phosphate and 200 mM NaCl, at pH 6. The proteins were found to be ∼95% pure as analyzed by sodium dodecyl sulfate polyacrylamide gel electrophoresis.

Size Exclusion Chromatography (SEC). The SEC experiment was performed using a Superdex-75 PG (prep grade, HiTrap 16/600) column mounted on an AKTA prime FPLC system, GE Healthcare. The Hup protein (WT and P64A) samples (1 mL each of 0.5 mM) were loaded on to column equilibrated with buffer (50 mM sodium phosphate, 200 mM NaCl, at pH 6) at 25 °C. The protein flow rate in SEC was kept as 1 mL/min and the eluted protein was analyzed by measuring absorbance at 215 nm using zinc lamp. The gel filtration profile of Hup proteins (WT and P64A) was compared with those of chymotrypsin (25 kDa) and pepsin (34.5 kDa as molecular weight references.

Circular Dichroism (CD) Spectroscopy. Far-UV CD experiments were performed on Hup protein (WT and P64A) samples (40 μM) using a Jasco J-1500 CD spectrometer at 25 °C. CD spectra of proteins were obtained in the wavelength range 190−250 nm with 1 nm resolution using a quartz cuvette of 1 mm path length.

Fluorescence Spectroscopy. Tertiary structural changes in Hup protein (WT and P64A) samples (40 μM) were probed by steady state fluorescence conducted on a Fluorolog$^+$ spectrometer (HORIBA JOBIN YVON, Japan). The samples were analyzed by exciting Tyr residue (intrinsic fluorophore) at 280 nm and recording fluorescence emission in the range of 285−400 nm at scanning speed of 1 nm/s. For ANS (8-anilinonapthalene-1-sulfonic acid) binding experiments, ANS (extrinsic fluorophore) was excited at 380 nm and the emission profile was obtained in the range of 400- 650 nm.[31,32] The excitation/emission slit widths were set at 5 nm for all the experiments.

Urea-based denaturation study was performed using Hup protein (WT and P64A) samples (40 μM) with urea ranging from 0 to 8 M (at 0.4 M interval). The concentration of urea was ascertained using the refractive index method.[33] The maximum intensity values for each sample as observed at 306 nm were normalized and further used to obtain protein unfolding curve. The curve was fitted to a two state model (D ↔ 2U) to obtain free energy (ΔG) values as explained previously.[14,34,35]

Fluorescence based quenching experiments were performed by titrating hairpin DNA (hp-DNA) to Hup protein (WT and P64A) samples (40 μM) at 25 °C. The nucleotide sequence of the hp-DNA is 5′ TTTTTTTTTTCGAAGAAAAAAAAAA 3′. The change in fluorescence maxima of Tyr residue at 306 nm was monitored throughout the experiment by sequential addition of hp-DNA. The binding parameters were discerned using the Stern−Volmer relationship by analyzing the double log plots.[36,37] All of the biophysical experiments were repeated twice for reproducibility. The DNA binding isotherms and Hup stability curves were plotted by considering the average of two measurements.

DNA Binding Assay. DNA binding assay was performed to understand binding of both Hup protein (WT and P64A) samples with hairpin DNA using Agarose gel electrophoresis method. Both Hup-WT and Hup-P64A samples were incubated with hairpin DNA for 10 min at 25 °C prior to loading on gel. Agarose gel was imaged on gel documentation system (Biorad) using Imagelab software and the experiments were repeated twice for reproducibility.

Nuclear Magnetic Resonance (NMR) Spectroscopy. Hup protein (WT and P64A) samples (∼0.5−1.0 mM) uniformly labeled with ^{13}C and/or ^{15}N were used to acquire NMR spectroscopy experiments on 500/800 MHz Bruker Avance NMR instrument. 2D-$^1H-^{15}N$ heteronuclear single quantum coherence (HSQC) spectra were acquired with carrier frequencies at 4.68 and 117 ppm and spectral widths of 12 and 34 ppm for ^1H and ^{15}N nuclei, respectively. 3D NMR experiments were acquired with ^{13}C carrier frequencies as 176 ppm for HNCO, 54 ppm for HNCA, and 43 ppm for HNCACB experiment. Secondary structural preferences of P64A protein were obtained by calculating the deviation in $^{13}C\alpha$ and $^{13}C'$ chemical shift values between the observed shifts (δ_{obs}) and random coil shifts (δ_{rc}) values. Cumulative chemical shift indices ($\Delta\delta^{CUM}$) were calculated using the following equation to predict the secondary structure information and were compared with the Hup-WT protein (BMRB NO: 26942).

$$\Delta\delta^{CUM} = \frac{\Delta\delta(C^{\alpha})}{25} + \frac{\Delta\delta(C')}{10}$$

Peak shifts as observed in the $^1H-^{15}N$ HSQC spectra of Hup-WT and Hup-P64A proteins were compared by calculating the chemical shift perturbation values using the following equation:

$$\text{chemical shift perturbation(CSP)} = \sqrt{(\Delta\delta H)^2 + \left(\frac{\Delta\delta N}{5}\right)^2}$$

Temperature-dependent changes were measured by recording $^1H-^{15}N$ HSQC spectra in the temperature range 293−308 K (regular interval of 3 K) on Hup protein (WT and P64A) samples (1 mM). The chemical shift value of amide proton corresponding to a particular residue were plotted and fitted with a linear regression model.[38] The native state hydrogen−deuterium exchange (H/D exchange) experiment was performed on lyophilized Hup proteins (∼1.0 mM, 25 °C) redissolved in 100% D_2O. Briefly, Hup protein samples (WT and P64A) were flash frozen in liquid nitrogen for 10−15 min, and then lyophilized for ∼10−12 h. For reconstituting protein sample, 100% D_2O was added to obtain a buffer composition 50 mM sodium phosphate, 200 mM NaCl at pH 6. The dead time (time interval between addition of D_2O and acquisition of HSQC spectra) for the experiment was ∼10 min.[39]

Backbone ^{15}N relaxation dynamics of P64A protein (1.0 mM) were studied using longitudinal relaxation R_1, transverse relaxation R_2 and $^1H-^{15}N$ steady state NOE (Het-NOE). Briefly, the R_1 relaxation delay parameters were 20, 60, 100, 200, 300, 400, 500, 600, and 800 ms, whereas the R_2 delays were kept at 10.56, 21.12, 31.68, 42.24, 52.8, 63.36, and 73.92 ms. In Het-NOE experiments, the saturation time and

https://doi.org/10.1021/acsomega.2c01754
ACS Omega 2022, 7, 15231−15246

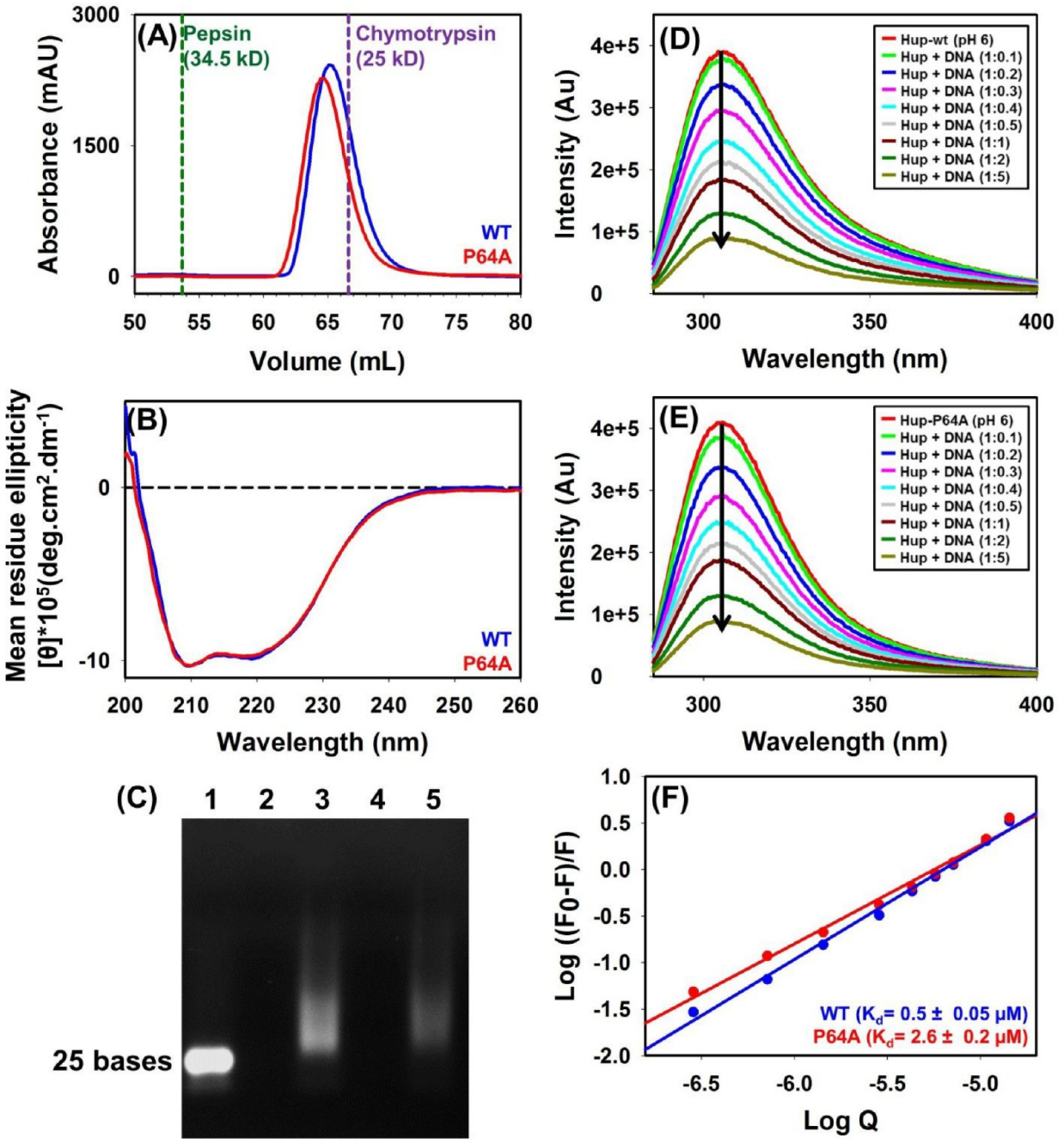

Figure 2. Biophysical characterization and DNA binding assay of Hup proteins (WT and P64A): (A) SEC profile of Hup proteins (WT, blue and P64A, red) compared with that of chymotrypsin (purple line, MW 25 kD) and pepsin (green line, MW 34.5 kDa) as standard reference proteins. (B) CD spectroscopy profile of Hup proteins (WT, blue and P64A, red) depicting the secondary structural characteristics. (C) Interactions between DNA and Hup proteins (WT/P64A) observed by agarose gel electrophoresis showing hp-DNA (25 bases, lane 1), WT:hp-DNA complex (lane 3), and P64A:hp-DNA complex (lane 5). Fluorescence quenching experiments showing a gradual decrease in fluorescence from WT protein (D) and P64A protein (E) after sequential addition of hp-DNA to obtain Hup:hp-DNA complex in molar ratio ranging 1:0.1 to 1:5. (F) Double logarithimic plots depiciting the dissociation constants (K_d) values for interaction of WT:hp-DNA (blue) and P64A:hp-DNA (red).

relaxation delay for proton were kept at 3.0 s, respectively. Only the peaks with considerable resolution were selected for relaxation analysis, and the relaxation properties were analyzed as reported earlier for the Hup-WT protein.[30] The error values in the NOE were analyzed as described elsewhere.[40] Topspin 3.6.1 software was used to acquire/process/analyze the NMR spectra and Computer Aided Resonance Assignment (CARA, version 1.8.4) software was used for backbone resonance assignment of Hup-P64A variant (BMRB No.: 51341).

Molecular Dynamics (MD) Simulation. The homology modeled Hup protein as reported previously (PMDB accession ID: PM0084232) was used as a starting template for the MD studies.[14,30] The model with the modification Pro to Ala was produced using PYMOL graphics software. All MD studies were performed with GROMACS 2020.5 version at pH 6. Briefly, MD simulation for Hup-P64A protein was performed at pH 6 with protonation states being defined using PROPKA3 and H^{++} server.[41] The protonation states were assigned with

https://doi.org/10.1021/acsomega.2c01754
ACS Omega 2022, 7, 15231−15246

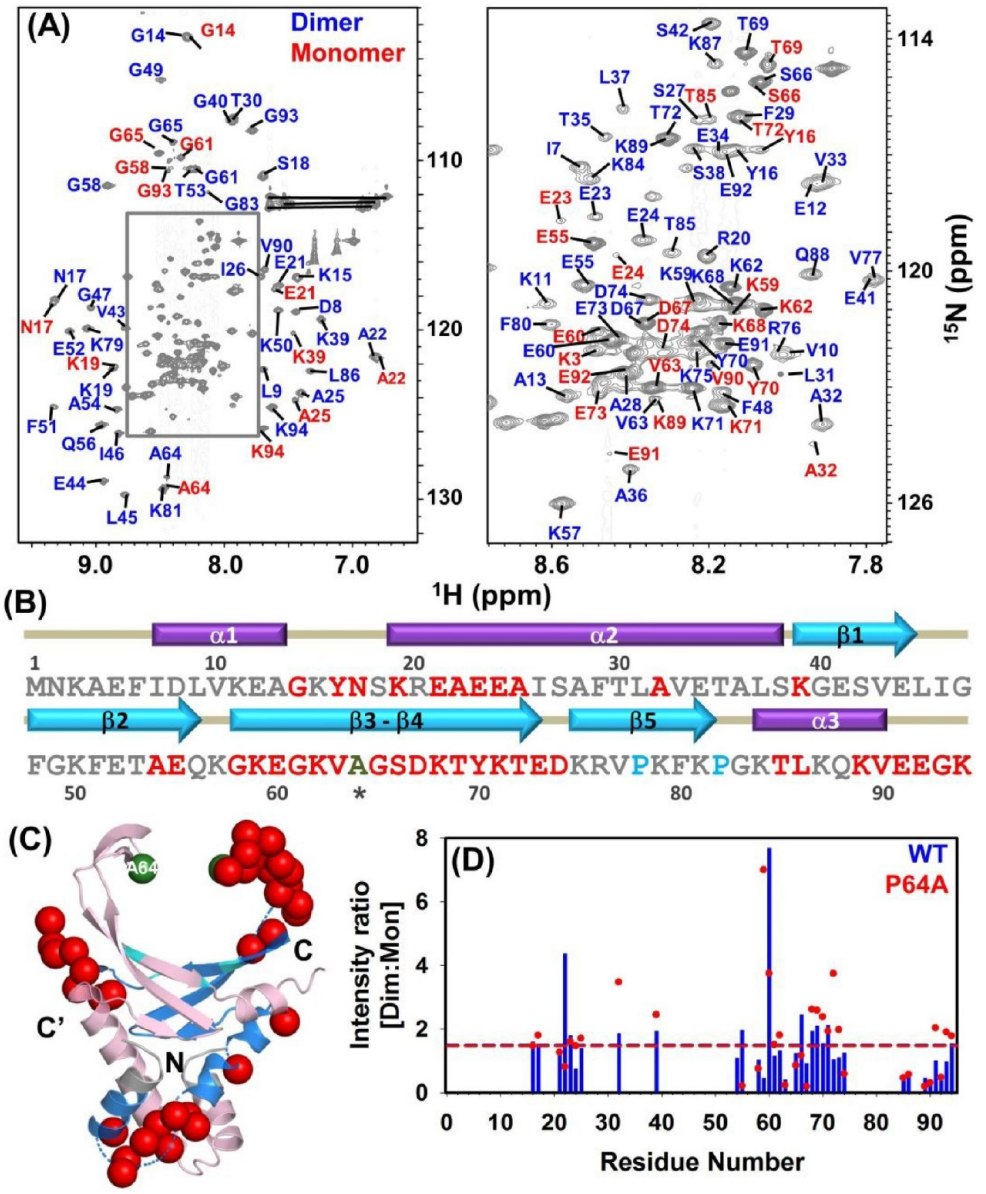

Figure 3. Backbone resonance assignment of Hup-P64A protein using NMR spectroscopy: (A) 2D- ^{1}H−^{15}N HSQC spectra of Hup-P64A mutant with annotated backbone amide signals. The residues belonging to the dimeric (D) conformation and the monomeric (M) conformation are marked with blue and red color, respectively. (B) Primary sequence of protein showing the assigned monomeric (M) residues, proline residues and mutated residue (marked with an asterisk, *) are highlighted in red, cyan and green, respectively. (C) Residues present in both dimeric and monomeric conformation are represented as red spheres on a monomer subunit of three-dimensional structure of Hup dimer generated by PYMOL software. The mutated residue A64 (P64A) is represented as green sphere. (D) Residue wise intensity ratio of dimer and monomer conformation of Hup proteins (WT, blue and P64A, red).

the help of the *inter* module of the *pdb2gmx*.[42,43] Protein topologies were generated using the Amber99sb-ILDN force field, and TIP3P solvation was performed in a cubic box.[42,43] After solvation, chloride ions were introduced into the protein environments to mimic the cellular milieu. The steepest descent algorithm-based energy minimization was performed for 5000 steps and a force cutoff value <1000 kJ/mol/nm.[44] Furthermore, the equilibration phase was carried out for 10 ns. Berendsen's weak coupling method and the Parrinello−Rahman barostat method were used to maintain the temperature and pressure of the system at 300 K and 1 bar, respectively, during *NVT* and *NPT*.[60,61] The final MD production was carried out for 500 ns with a time step equal to 2 fs, and the constraints were applied using the LINCS algorithm. The trajectory parameters such as root-mean-square deviations (RMSD), the radius of gyration (R_g), root-mean-square fluctuations (RMSF), and solvent accessibility surface area (SASA)[44,45] were obtained and compared with WT protein at pH 6 as reported earlier.[14]

Multiple Sequence Alignment and Phylogenetic Analysis. HU protein sequences from 58 different organisms belonging to Firmicutes (23), Proteobacteria (19), Cyanobacteria (3), Bacteroides (2), Thermotoga (1), Bacteriophages (7), and Plantae (3) were obtained from the UniProt database. The sequences were aligned using MUSCLE algorithm integrated in MEGA software.[46] The phylogenetic analysis was performed using neighbor joining (NJ) method, with the *p*-distance model, the number of threads equal to four, and a

https://doi.org/10.1021/acsomega.2c01754
ACS Omega 2022, 7, 15231−15246

bootstrap value of 1000. The phylogenetic tree thus obtained was modified using iTOL web server.[47] The conservation profile of the aligned HU protein sequences was prepared using Web logo server.[48]

RESULTS

Assessing the Global Structural Features and DNA Binding Potency of Hup-P64A Protein. To study the regulatory role of Pro (P64) residue on structure and function of Hup protein, P64A mutant was generated using site-directed mutagenesis (Figures S1 and S2), and the recombinant protein was overexpressed, purified and visualized using sodium dodecyl sulfate polyacrylamide gel electrophoresis (Figure S3). As Hup protein exists as a dimer in solution, SEC experiment was performed to assess the oligomeric state of the P64A. As depicted in Figure 2A, P64A protein eluted at the same fractions to that of WT protein, thus suggesting for a similar oligomeric state (dimer) at given experimental conditions. In general, substitutions/insertion/deletion of amino acids in terms of point mutations can lead to certain extent of secondary/tertiary structural changes. Secondary structural changes of P64A protein monitored by far UV-CD experiments (Figure 2B), and the tertiary structural changes observed using the intrinsic fluorophore (Tyr) (Figure S4), indicated for undeterred secondary/tertiary structural features to that of WT protein. The SEC, CD, and fluorescence results established that the overall structural and oligomeric features of P64A are conserved, thus designating the selected variant as a promising probe to investigate the functional competence of P64 residue in Hup protein.

In order to dissect the role of P64 in DNA binding interaction of Hup protein, DNA binding assays were performed using agarose gel electrophoresis and fluorescence spectroscopy (Figure 2C−E). It is worth noting that HU protein nonspecifically binds to dsDNA, RNA, and DNA-RNA hybrids, and it does prefer A/T-rich regions in the substrate.[49−51] Hence, the hp-DNA with A-T repeats was chosen in the present study to characterize the Hup-DNA interaction. In agarose gel assay, addition of hp-DNA to Hup proteins (WT and P64A) showed smearing of DNA [lane 3 and lane 5], thus indicating that P64A protein is also functionally competent (Figure 2C). Henceforth, to quantitate the binding of Hup proteins (WT and P64A) with DNA, fluorescence quenching experiments were performed (Figure 2D,E). Binding of Hup protein with DNA resulted in fluorescence quenching due to alteration of Tyr residues' environment at the DNA binding pocket (Figure S4).[14] As expected, significant changes in fluorescence intensities have been observed after sequential addition of DNA to Hup proteins (WT and P64A) (Figure 2D,E). The dissociation constant (K_d) values calculated using double log plots were 0.5 ± 0.05 μM for WT and 2.6 ± 0.2 μM for P64A protein, thus indicating for a differential DNA binding (Figure 2F). Comparison of K_d values clearly evidenced that the binding of P64A protein is five times lower to that of its WT counterpart, thus signifying the functional role of apical proline residue (P64) in HU protein of *H. pylori*. The observed attenuation in the DNA binding properties of P64A can be attributed to (i) direct loss of interacting P64 side chain, (ii) structural/dynamic alterations in the DNA binding pocket of Hup, and (iii) a combination of both points i and ii, as Pro residue is known to significantly alter the conformational/dynamics/stability aspects of the proteins.[52,53] In order to probe these aspects, the structural, stability and dynamic characteristics of P64A has been dissected at atomic level using protein NMR experiments and compared with WT protein in the following sections.

Backbone Resonance Assignment of Hup-P64A Protein. Hup protein is known to exhibit conformational heterogeneity in terms of monomer−dimer equilibrium, as resonances of both species under the slow exchange of the NMR time scale are observed in the $^{1}H-^{15}N$ HSQC spectrum.[14,30] To unravel such conformational heterogeneity and/or resemblance in P64A, a 2D-HSQC spectrum was recorded. The analysis of the $^{1}H-^{15}N$ HSQC spectrum revealed significant difference in the amide cross peak pattern (Figure S5). Therefore, the direct transfer of assignment was not feasible from WT to P64A protein. Hence, 3D NMR experiments were performed to unambiguously assign amide resonances of P64A protein. Likewise Hup-WT protein at pH 6, P64A protein also showed more than ∼140 peaks in the $^{1}H-^{15}N$ HSQC spectrum (Figure 3A). In comparison to WT protein, where 85 peaks for the dimer and 48 peaks for the monomer conformation were assigned, the backbone resonance assignment of P64A resulted in assignment of 86 peaks corresponding to dimer conformation and 38 peaks representing the monomer conformation (Figure 3A). A representative HNCACB sequence walk for residues E60-G65 accessing both dimer and monomer states has been presented in Figure S6. The summary of all the assigned residues and residues undergoing dimer−monomer transition have been marked on the amino acid sequence of P64A protein (Figure 3B). The observed resonances corresponding to the monomeric conformation were predominantly in the C-terminal half, i.e., preferably in the region forming the β-arm of P64A protein, which is in line with that of WT protein (Figure 3C). Furthermore, to assess whether the P64A mutation is altering the dimer to monomer population dynamics of Hup protein, a residue wise intensity ratio of dimer and monomer conformations was calculated for Hup proteins (WT and P64A) (Figure 3D). It has been observed that the cumulative average of intensity ratio for [dimer:monomer] of both the Hup proteins (WT and P64A) are ∼1.5 at 298 K, thus suggesting that P64A does not alter the monomer−dimer equilibrium of Hup protein. Considering the location of P64, it is anticipated that it should not influence the oligomerization characteristics of Hup protein, which is in line with the observed experimental evidence. Although the monomer−dimer equilibrium is unaffected, the observed changes in the amide resonances can point toward the possibility of some secondary/tertiary structural changes at few segments in the P64A protein (Figure S5).

Dissecting the Structural Features of Hup-P64A Protein. *Secondary Structure Preferences of P64A Protein.* The position of substituted proline may influence the secondary structural elements in the vicinity as Pro residue is known to introduce kinks in the β-sheet regions. Thus, to infer the secondary structural changes due to proline substitution, chemical shift indices ($\Delta\delta^{CUM}$) were obtained for both the dimer and the monomer conformations of the P64A protein and compared with those of the WT protein (Figure 4A,B). The secondary structural preferences for dimeric WT protein shows two initial α-helices (α1 and α2), with interspersed loop region followed by five β-strands and another α-helix (α3) at the end. In P64A, all the α-helices show similar structural preferences as observed for dimeric state of WT protein,

https://doi.org/10.1021/acsomega.2c01754
ACS Omega 2022, 7, 15231−15246

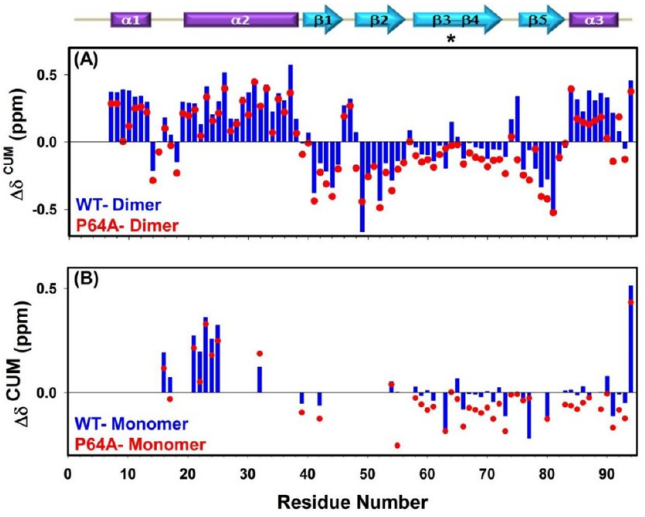

Figure 4. Secondary structural preferences of Hup proteins (WT and P64A) estimated using NMR spectroscopy. Residue-wise comparison of cumulative secondary chemical shifts indices ($\Delta\delta^{CUM}$) of Hup proteins (WT, blue bar and P64A, red spheres): (A) dimeric conformation; (B) monomeric conformation. The secondary structure preferences for P64A protein are shown at the top as an arrangement of α-helix (purple bar), and β-strand (cyan arrow) with mutated P64 residue (marked with an asterisk, *).

however, notable changes were predominant in the β-strand region. Although, the β1, β2, and β5 strands remain unaltered showing similar structural propensities as compared to WT protein, interestingly, β3 and β4 strands were observed to be extended (Figure 4A). This extension of β3 and β4 strands in the absence of P64 can be attributed to the substitution of proline to alanine, as the former results in termination of the β-strand. Earlier, it has been reported that in case of monomer conformation of WT protein the N-terminal helical region (α1 and α2) were similar to that of the dimer, whereas the C-terminal half comprising of β-strands and α3 is unstructured as is evident from the chemical shift indices ($\Delta\delta^{CUM}$) (Figure 4B).[30] Contrarily, in case of P64A, the C-terminal half is observed to attain same structural attributes, as the residues show extended β-strand preferences in β3−β5 region. From both the secondary structural preferences of monomeric and dimeric Hup, it is evident that P64A significantly influenced the structural preferences in the β-strand region (β3-β5). Such secondary structure changes in general accompany tertiary structural changes (local/segmental) as a result of perturbation in N−H bonds. Therefore, to substantiate the altered secondary structural preferences and unravel the presence of preferred tertiary structural changes, the amide bond perturbations have been assessed.

Chemical Shift Perturbation (CSP) Analysis of the P64A Protein. A closer look at the $^{1}H-^{15}N$ HSQC spectrum of P64A protein suggested significant peak shifts for the residues that are far away from the site of substitution (Figure 5A, Figure S5). Henceforth, to quantitate the observed changes across the polypeptide chain, the chemical shift perturbations (CSP) were calculated. CSPs are net resultant sum of deviations in both ^{1}H and ^{15}N dimensions and hence, used to obtain quantitative estimate of perturbations for each residue. For dimeric P64A protein, the residues belonging to the β1−β5 and C-terminal end showed very high CSP values, predominantly those in the β3 and β4 region, suggesting severe amide perturbation in this region (Figure 5B). Although, the number of residues observed was less, similar trend was obtained for residues of monomeric conformation. The residues showing significant CSP values for both dimeric and monomeric P64A protein were mapped on the 3D structure of Hup-P64A protein (Figure 5C). The perturbed residues (G58, K59, K62, V63, G65, S66, and D67) were found to be clustered at the site of mutation, and there after dispersed in to residues of β-arm region (A54, E55, E73, K75, and V77). Furthermore, long-range perturbations were also observed due to relay of three-dimensional interaction network, as evident for the CSP changes observed for the residues (K19, E21, L37, S38, E41, L45, F51, T85, L86, K89, and E91) in the DD. The CSP network map established that the P64 not only influence the local structural preferences of Hup protein around β3−β4 strands, but also regulate the long-range interaction networks that are involved in DNA binding (Figure 2C). As these local structural perturbations can influence the H-bonding of the participating amino acids, the resultant H-bonding patterns were also analyzed.

Analyzing the Hydrogen-Bonding Preferences of the P64A Protein. Temperature coefficients derived from the amide proton chemical shifts provide a legitimate estimate of H-bonding and local stability of a protein. H-bonded amide proton has a temperature coefficient value >−4.5 ppb/K, it is in the range of −5 to −12 ppb/K for the unstructured region, and it is around −18 to −30 ppb/K when involved in transient H-bonding.[54,55] The residue-wise amide proton temperature coefficients of dimeric Hup proteins (WT and P64A) indicated that temperature coefficient for residues in α1, α2, α3, β1, and β5 ranged in between 0 and −4.5 ppb/K, indicating their H-bonded nature. However, very low temperature coefficients ranging from −5 to −15 ppb/K for residues in the β3 and β4 region, suggesting the lack of stabilizing H-bonds (Figure 6A,B). In line to these observations, the residues of monomer in β3 and β4 region showed very low temperature coefficients, suggesting their non-hydrogen-bonded nature (Figure 6A,B). Interestingly, six residues (S18, K39, E41, F48, G61, and G93) in both WT and P64 dimeric proteins showed positive temperature coefficients due to induced ring current effects.[54]

To analyze the residues contributing to differential temperature coefficients/H-bonding patterns, a correlation map between the temperature coefficient values of Hup dimeric/monomeric proteins (WT and P64A) were prepared as reported previously.[56] Comparison of dimer and monomeric conformation of Hup proteins (WT and P64A) revealed differential temperature coefficients for ∼11 amino acids in dimer and ∼8 residues for monomer conformation (Figure 6C,D). Out of 11 residues observed for the dimer, three residues (D67, Y70, and E73) were present near the site of P64A substitution at the β-arm region; thereafter, six residues were present in the dimerization domain (L31, A36, F48, K50, V77, and K81) and two at the C-terminal end (K89 and E92) (Figure 6E). Similar analysis for monomer conformation suggests that six residues (G58, V63, G65, S66, K68, and D74) were majorly present near site of P64A substitution in β3-β4 region and rest two were found to be in the dimerization domain (E24) and at the C-terminal end (E91) (Figure 6E). All these observations point that the structural perturbation has been relayed toward the saddle pocket and dimerization domain (DD) from the site of P64A substitution, which echo the CSP results. Such structural changes can indeed alter the local/global stability of the Hup molecule.

https://doi.org/10.1021/acsomega.2c01754
ACS Omega 2022, 7, 15231−15246

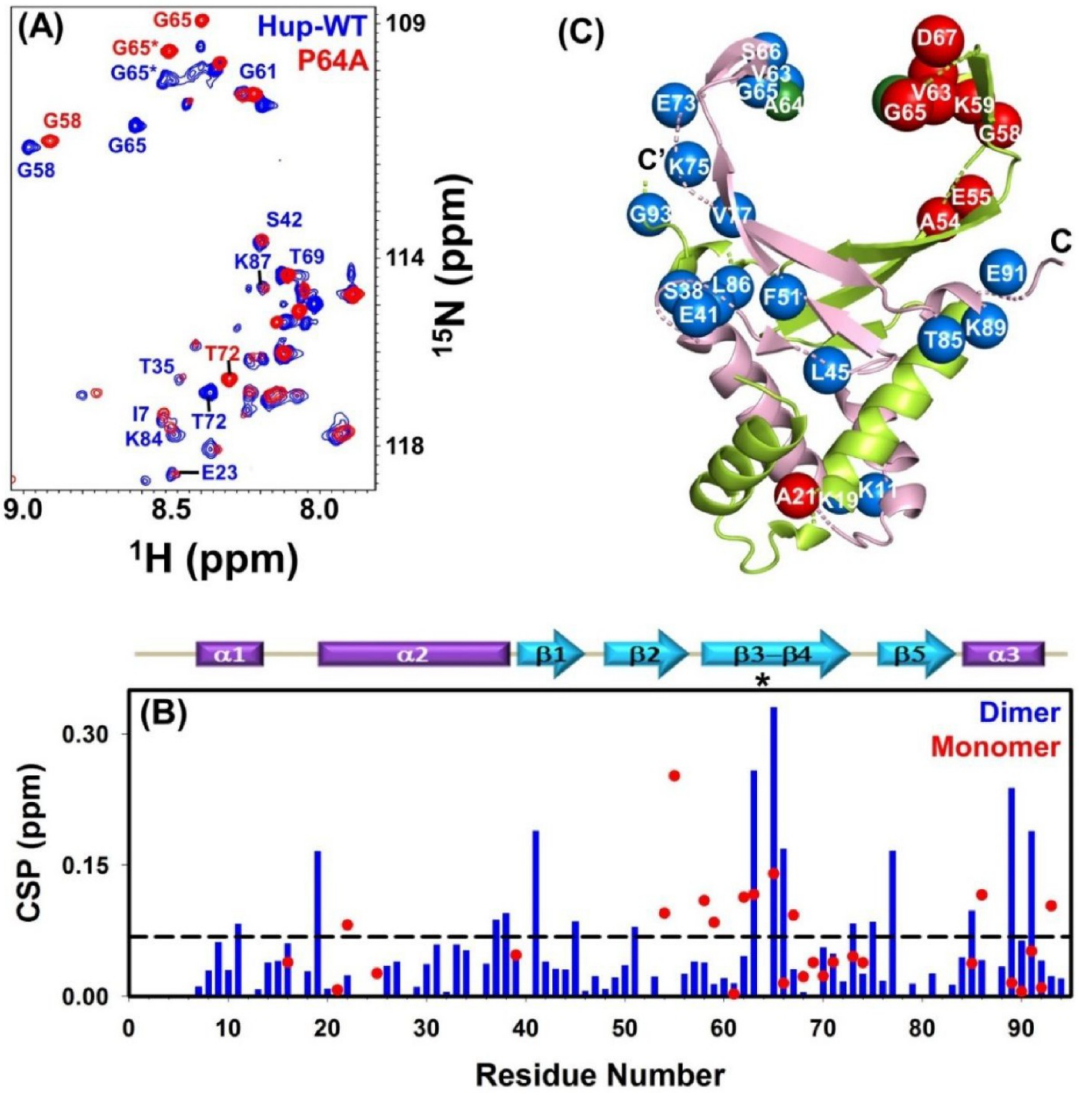

Figure 5. Comparative chemical shift analysis of Hup proteins (WT and P64A). (A) Selective overlay of ^{1}H−^{15}N HSQC spectra of Hup proteins (WT, blue and P64A, red) showing peak shifts. (B) Chemical shift perturbations observed in the P64A protein dimer (blue bar) and monomer (red dots) due to the P64A mutation in the Hup protein. The cutoff value of chemical shift was decided on the basis of average chemical shift perturbation value and is denoted by black dotted line (∼0.8 ppm).The secondary structure preferences for P64A protein are shown at the top as an arrangement of α-helix (purple bar), and β-strand (cyan arrow) with mutated P64 residue (marked with an asterisk, *). (C) Residues showing significant chemical shift perturbations greater than average cutoff value are represented as spheres (Dimer, blue, and monomer,red) on different monomeric subunit of three-dimensional structure of Hup dimer generated by PYMOL software. The mutated residue A64 (P64A) is represented as green sphere.

Structural Stability Aspects of Hup-P64A. In order to assess whether the structural perturbations observed in the P64A protein can affect the stability/protection of backbone amide protons, the NMR spectroscopy based hydrogen−deuterium (H/D) exchange experiment was performed with a dead time of ∼10 min. Amide protons that are exposed to the solvent and/or not involved in H-bond/structure formation exchange faster with the deuterium.[57] The H/D exchange spectra of Hup proteins (WT and P64A) showed ∼27 protected residues for the WT protein and ∼36 protected residues for the P64A protein (Figure 7A,B). The protected residues were marked on the sequence (Figure 7C) and on three-dimensional structures (Figure 7D,E) of the Hup proteins (WT and P64A). For both WT and P64A proteins, a majority of the protected residues were located in the dimerization domain [23 of 27 for WT and 27 of 36 for P64A] formed by the α1, α2, and β1 region. Indeed, such a high extent of protection at the dimerization domain (DD) is anticipated considering the fact that the hydrophobic core of the dimerization domain (DD) is involved in stabilizing the Hup protein, and is considered as hotspot of unfolding as reported by NMR studies.[14] Further, the proteins showed differential number of protected residues in β-arm region near to the site of P64A mutation, i.e., 4 for WT protein and 9 for P64A protein. Overall, the residues showing differential protection were found to be four (N17, T35, V43, and K81) in the dimerization domain (DD), seven (G61, K62, V63, A64, G65, T69, K71) in the β3−β4 strand forming β-arm region, and three (K84, T85, and K94) at the C-terminal end of the WT and P64A proteins (Figure 7D,E). Such a differential/enhanced protection of NH bonds in the P64A protein can either contribute to the local/segmental stability or else can

https://doi.org/10.1021/acsomega.2c01754
ACS Omega 2022, 7, 15231−15246

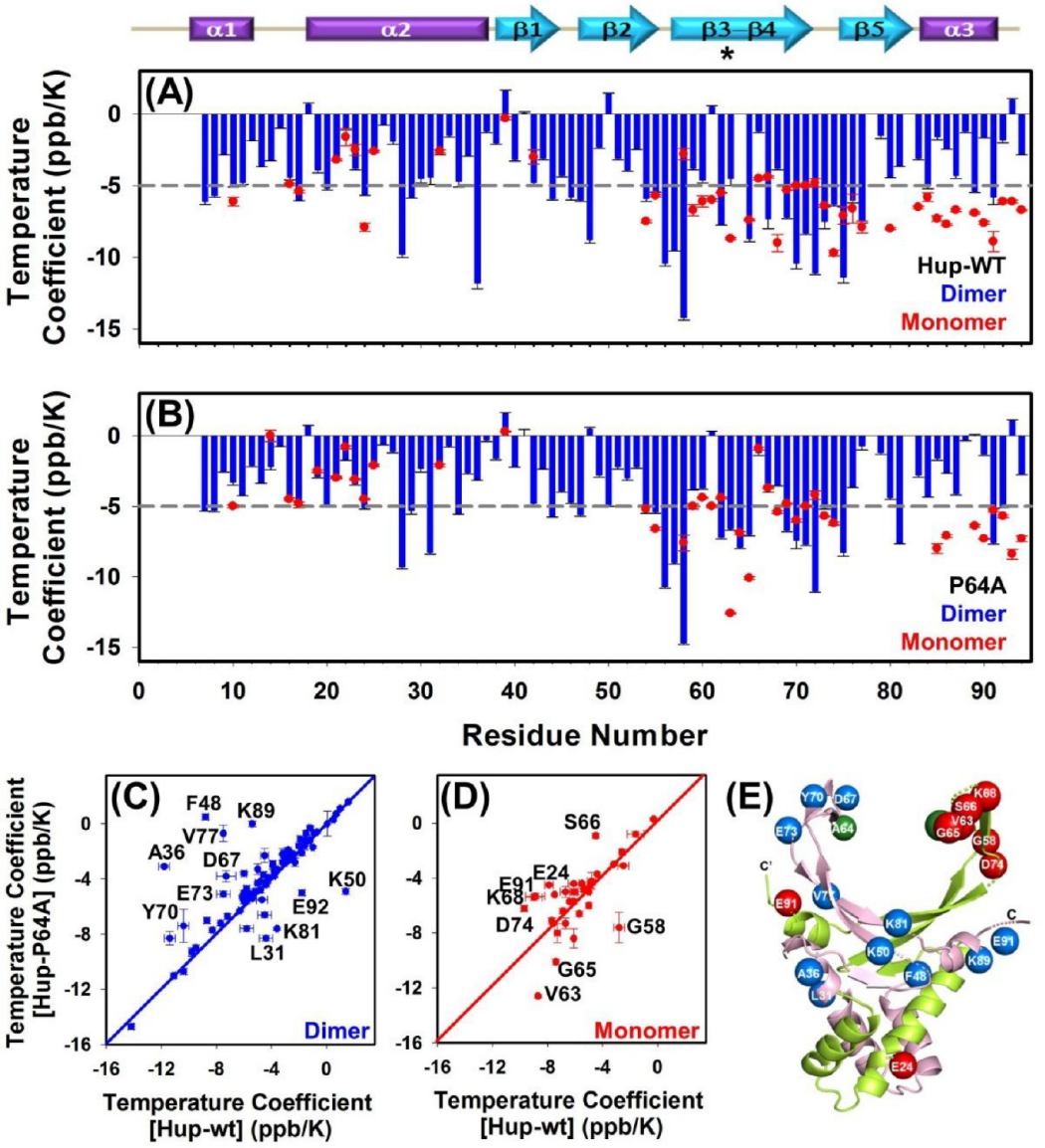

Figure 6. Temperature dependent structural changes in Hup proteins (WT and P64A). Residue-wise temperature coefficients of (A) WT protein dimer (blue) and monomer (red) (B) P64A protein dimer (blue bar) and monomer (red dots). The secondary structure preferences for P64A protein are shown at the top as an arrangement of α-helix (purple bar) and β-strand (cyan arrow) with a mutated P64 residue (marked with an asterisk, *). Correlation map between temperature coefficients of Hup proteins (WT and P64A): (C) dimer and (D) monomer. (E) Residues showing the deviation of >2 ppb/K from the diagonal are represented as spheres (dimer, blue; monomer, red) on the three-dimensional structure of Hup dimer generated by PYMOL software. The mutated residue A64 (P64A) is represented as green sphere.

alter the global stability of Hup protein. To further evaluate this, fluorescence-based urea denaturation studies were performed on WT and P64A proteins (Figure S7). The unfolding curves evidenced for similar unfolding free energies [$\Delta G = -5.0 \pm 0.2$ kcal/mol for WT and $\Delta G = -4.7 \pm 0.3$ kcal/mol for P64A] and transition midpoints [$Cm = 1.6 \pm 0.1$ for WT, and $Cm = 1.5 \pm 0.1$ for P64A], thus establishing that the observed differential protection in P64A protein only contributes to local/segmental stabilities, without altering the global stability of the Hup protein (Figure S7C, Table S2).

Evaluating the Conformational Dynamics of the Hup-P64A Protein. The altered structural/stability characteristics of P64A can be accompanied by altered conformational dynamics. Hence to elucidate the changes in conformational dynamics, molecular dynamics simulation studies and ^{15}N relaxation studies were performed on P64A, and are compared with its WT counterpart reported earlier.[14,30] The overall conformational stability and dynamics of the P64A protein was assessed by performing MD simulation studies for 500 ns. The comparative structural ensembles for Hup proteins (WT and P64A) at different time points were generated, and the observed structural fluctuations in the DNA binding domain (DBD) were shown in parts A and B of Figure 8. Over time, the WT protein showed higher conformational flexibility as compared to P64A protein. The RMSD values for WT protein (0.48 ± 0.1 nm) were stable up to 200 ns and showed fluctuations thereafter (Figure 8C). Strikingly, for entire 500 ns, the P64A protein showed stable RMSD (0.42 ± 0.1 nm), which is lower than that for the WT counterpart. The RMSF values were also observed to be lower for the P64A protein, suggesting decreased structural flexibility (Figure 8D). However, a significantly higher RMSF was observed for the

https://doi.org/10.1021/acsomega.2c01754
ACS Omega 2022, 7, 15231−15246

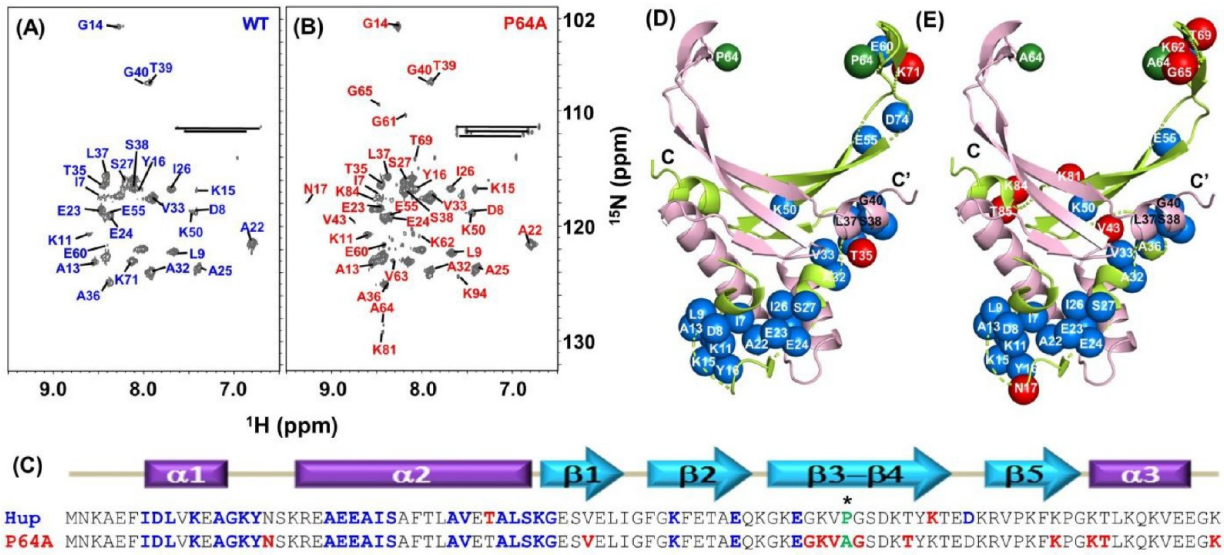

Figure 7. Stability analysis of Hup proteins (WT and P64A). ^{1}H−^{15}N HSQC spectra of Hup proteins (WT and P64A) depicting H/D exchange of (A) the WT protein and (B) the P64A protein recorded for 60 min with a dead time of 10 min. (C) Protected residues common for Hup proteins (WT and P64A) are marked with a blue color while those exclusive for a protein are marked with a red color on the primary sequence of Hup proteins (WT and P64A). The secondary structure preferences for P64A protein are shown at the top as an arrangement of α-helix (purple bar), and β-strand (cyan arrow) with mutated P64 residue (marked with an asterisk, *). Protected residues showing peaks in ^{1}H−^{15}N HSQC spectrum after 60 min have been marked on three-dimensional structure of Hup protein (D, WT and E, P64A). Protected residues common for Hup proteins (WT and P64A) are represented using blue spheres while those exclusive for a particular variant are represented using red spheres on one of the monomeric subunits of the Hup protein.

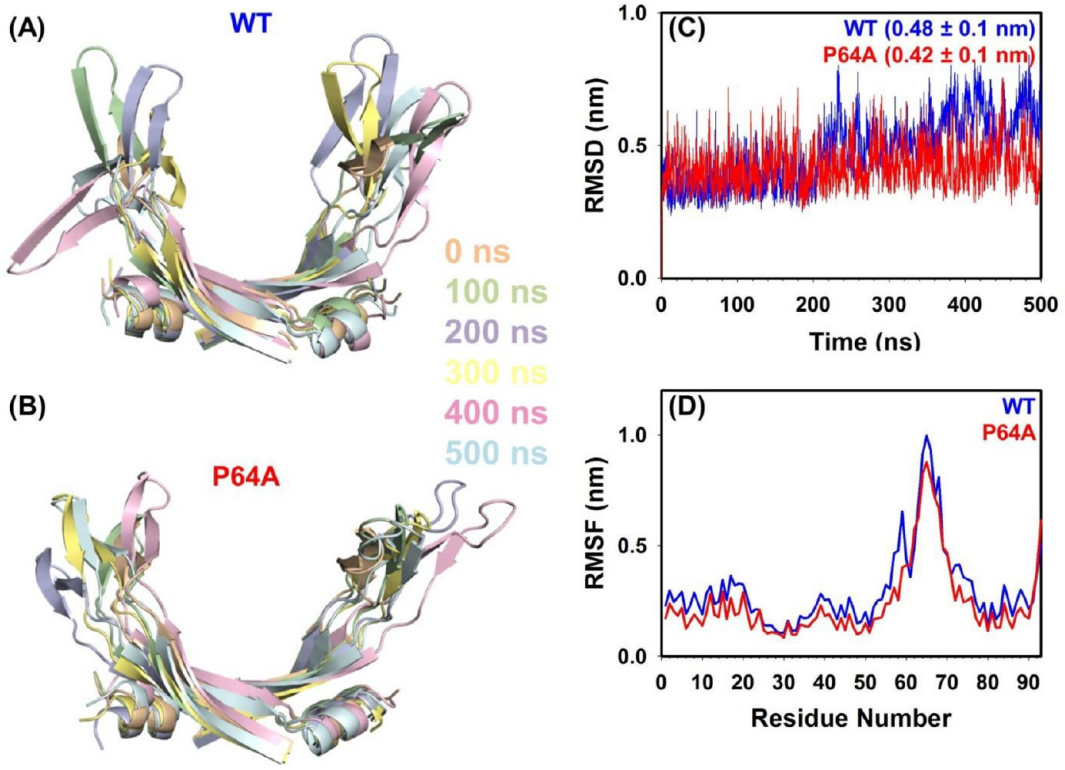

Figure 8. Conformational dynamics of Hup proteins (WT and P64A). Overlay of structural ensembles of Hup proteins obtained through MD simulation: (A) WT and (B) P64A showed differences in the β-arm region at various time intervals of the trajectory [0 ns, peach; 100 ns, green; 200 ns, purple; 300 ns, yellow; 400 ns, pink; and 500 ns, cyan]. Graphs representing the variation in RMSD over the time (C), and root-mean-square fluctuation (RMSF) (D) for each residue of the Hup (WT/P64A) proteins.

residues (K50 to Y70) that belonged to the β1−β4 region forming the DNA binding domain. Further, average radius of gyration (R_g) values and the solvent accessible surface area (SASA) showed no significant change suggesting for similar conformational features of both the Hup proteins, which is also

https://doi.org/10.1021/acsomega.2c01754
ACS Omega 2022, 7, 15231−15246

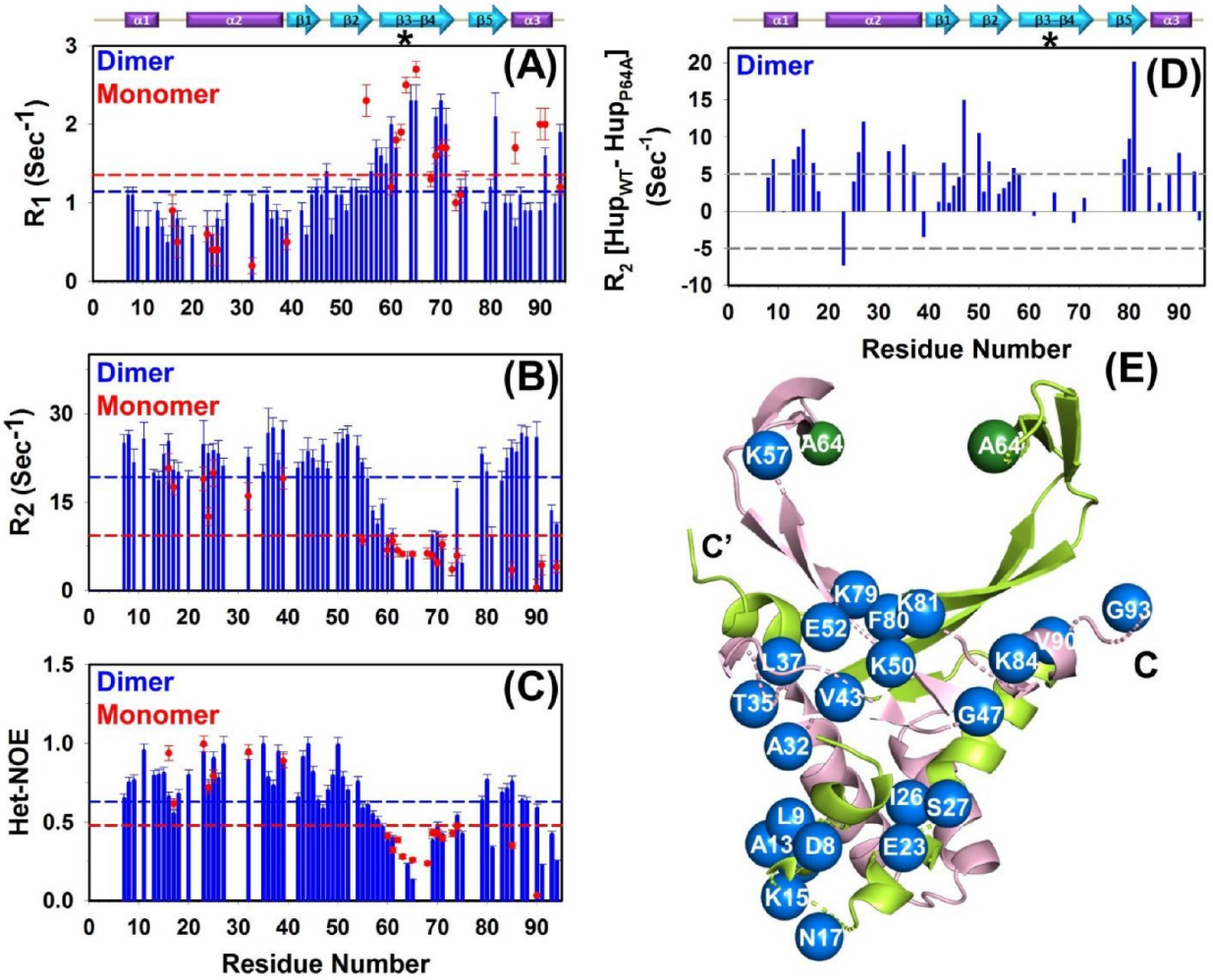

Figure 9. NMR-based ^{15}N relaxation analysis of Hup-P64A protein. Residue-wise overlay of longitudinal relaxation rates (R_1) (A), transverse relaxation rates (R_2) (B), and steady state Het-NOE (C), observed for the P64A protein (dimer, blue bar, and monomer, red dots). The transverse relaxation (R_2) difference value of Hup proteins (WT and P64A) (D), calculated for each residue. The secondary structure preferences for P64A protein are shown at the top as an arrangement of α-helix (purple bar), and β-strand (cyan arrow) with mutated P64 residue (marked with an asterisk, *). (E) Residues showing significant differential transverse relaxation, i.e., above the chosen cutoff value, represented as spheres (blue) on a monomer subunit of three-dimensional structure of Hup dimer generated by PYMOL software. The mutated residue A64 (P64A) is represented as green sphere.

evident from their similar ANS fluorescence spectral features (Figures S8 and S9).

To further substantiate the attenuation of overall conformational dynamics of the P64A protein and higher flexibility of the β1−β4 region forming the DNA binding region, NMR-based ^{15}N relaxation experiments were performed. All the three relaxation parameters such as the R_1, R_2 and steady state Het-NOE suggested that the P64A molecule is rigid in the N-terminal half as compared to its C-terminal counterpart. As evident from all the relaxation parameters such as higher R_1 values and lower R_2 and Het-NOE values, the β-strand region comprising of β2−β4 is highly flexible on the faster time scale (ns-ps) motions for both the dimeric and monomeric conformations measured (Figure 9A−C). Furthermore, to ascertain the effect of P64A mutation on Hup protein in terms of flexibility, and differential relaxation, difference in transverse relaxation rates of Hup proteins (WT and P64A) was calculated (Figure 9D). Herein, the ΔR_2 values clearly indicated that the WT protein was found to be more flexible than the P64A protein counterpart. The residues showing higher rigidity in the P64A protein were marked on the monomer subunit of a three-dimensional structure of the P64A protein (Figure 9E). The residues showing altered relaxation dynamics were spanned along the polypeptide chain. These observations are in concurrence with the MD simulation results, wherein the WT protein was found to be more flexible than the P64A protein.

DISCUSSION

Molecular Insights into the Altered Structural and DNA Binding Characteristics of the Hup-P64A Protein. Cellular processes such as DNA maintenance and chromosomal organization require periodic opening, closure, and diffusion in to the nucleic acids. Thus, DNA binding proteins (DBPs) or transcription factors (TFs) are expected to interact with the DNA with utmost fidelity. Owing to the very high functional relevance in the cellular responses certain segments of TF sequences remain conserved throughout all the domains of life.[58] Nucleoid associated proteins (NAPs) belonging to HU family have been found in Bacteria, Achaea, Eukarya

https://doi.org/10.1021/acsomega.2c01754
ACS Omega 2022, 7, 15231−15246

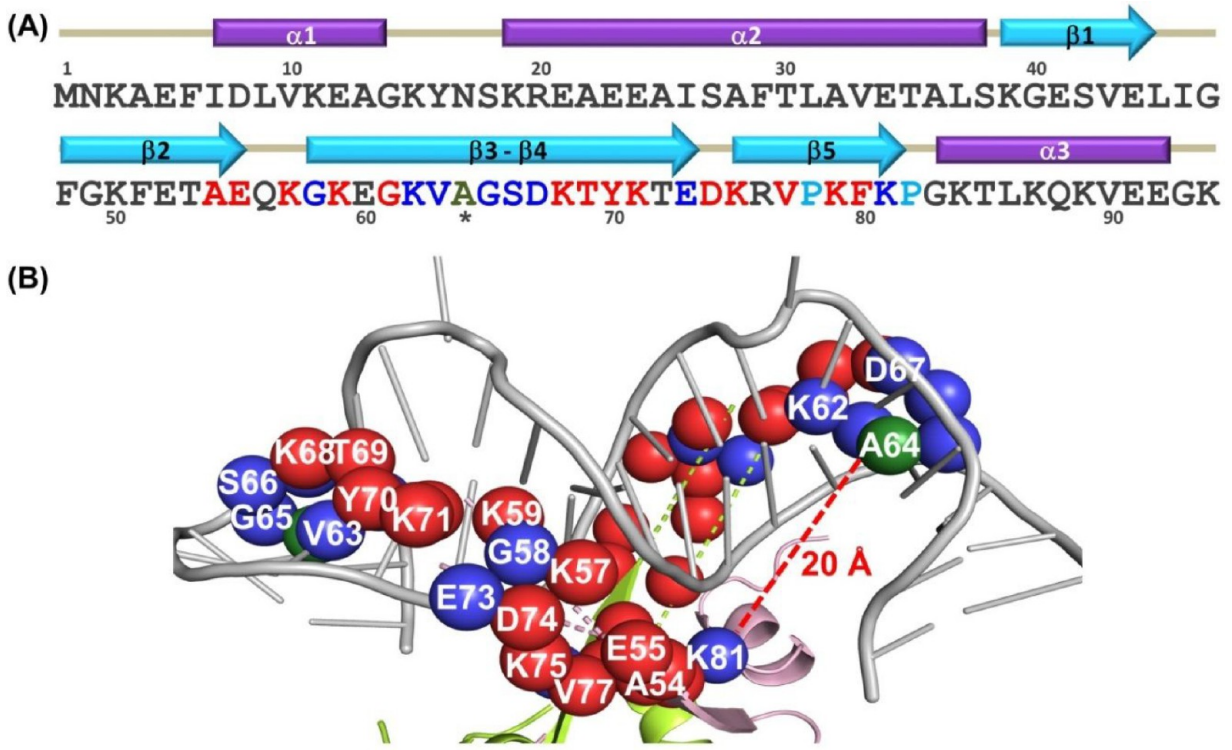

Figure 10. Summary of the residues exhibiting altered structural/stability/dynamics features in the DNA binding domain of Hup-P64A variant. (A) Residue-wise representation of perturbed residues in the β-arm region as determined using CSP, temperature coefficients, hydrogen exchange and relaxation analysis. (B) Residues showing perturbation shown as spheres on the three-dimensional structure of Hup dimer generated by PYMOL software. The mutated residue A64 (P64A) is represented as green sphere. The residues showing significant differences in one of the NMR parameter (CSP/temperature coefficient/hydrogen−deuterium (H/D) exchange/^{15}N relaxation) are represented with red color, whereas residues showing differences in more than one parameter, i.e., two or more are highlighted with blue color on both the sequence and the structure.

(primitive), plant chloroplasts, and bacteriophages.[59−61] HU family proteins seem to be evolutionarily related/conserved as evident from the phylogenetic tree (Figure S10), while possessing marginal sequence similarity score up to 37%.[22] In light of evolution, mutations and selection thereafter plays a decisive role in defining the split bifurcation of a lineage.[62] The members of HU family show high sequence polymorphism, albeit several residues show very high conservation rate along evolutionary lineage[13,22] (Figure S11). In all the families analyzed, the apical proline (P64, for Hup) has been observed to be fully conserved (Figure S11). Indeed, it is essential for Pro to remain conserved in order to regulate the structural stability and crucial functional competence of the HU protein(s) in terms of DNA binding.[13,19,20]

Conserved proline residues are considered vital for structural stability of protein as they play a crucial role in structure formation, oligomerization, peptide bond isomerization, protein engineering, protein−protein interactions, and so forth.[37,52,63,64] Hence, a change resulting in substitution of a proline can induce local/global structural/stability changes of the protein. In Hup protein proline (P64) regulates the conformational preferences of the β-turn connecting β3−β4 strand, thus aiding in termination/extension of these structural elements (Figure 4A). Such altered structural preferences resulted in localized tertiary structural changes as visualized by CSP analysis (Figure 5). Indeed, the influence of a proline on the protein structural integrity is largely dependent on the position and its local environment in the protein structure.[53] As observed for DsbA protein, the P151A mutation results in instability due to global rearrangement of the loop and loss of van der Waals interaction with nearby residues.[65] In P64A, ∼ 24 residues out of 31 residues (K50−81) forming the β-arm region are observed to exhibit structural/stability perturbation and conformational rigidity as evidenced from various NMR analysis (Figure 10A,B). All these alterations were found to be majorly concentrated in the DNA binding domain and do not alter the global stability of Hup protein. On a similar note, substitution (P135K) in human acidic fibroblast growth factor 1(hFGF1) leads to partial destabilization of protein structure in the β-arm region and at the base of the saddle pocket, without affecting its overall stability.[66] Moreover, it is interesting to note that the P64 is engaged in long-range contacts, as significant structural/stability fluctuations were observed up to 20 Å distance (Figure 10B). These perturbations can be attributed to introduction of otherwise absent amide moiety after replacement of Pro with Ala. Elimination of the pyrrolidine ring in case of *Thermotoga maritima* acetyl esterase resulted in the loss of van der Waals and hydrophobic interactions, leading to impaired activity and substrate specificity.[67] These observations further reconcile that the interactions in the dimerization domain (DD) play a central role in dictating the global stability of the Hup protein, and the β-arm region has a limited role or no role in the stability of the Hup protein as observed previously.[14]

The conserved nature of amino acid across lineages even after several bifurcations indicate their structural and/or functional relevance for the protein family *per se*.[68] For instance, proline is found to be conserved and crucial for the activity of several proteins like hypoxia-inducible factor-α (HIF-α),[69] Fpg glycosylase,[70] acetohydroxyacid synthase

https://doi.org/10.1021/acsomega.2c01754
ACS Omega 2022, 7, 15231−15246

(AHAS) of *Mycobacterium tuberculosis*,[71] and so forth. The mutations A100P and P191A in the TATA box region established the utility of proline in DNA binding where presence of proline was correlated to DNA binding affinity.[72] Also, DNA condensation by H1-histone was found to rely on proline containing a S/TPKK motif forming a β-loop.[73,74] Integration host factor (IHF) protein, a close contemporary to HU proteins introduces a kink in DNA where the Pro residue intercalates/wedges into a minor groove of DNA thereby introducing a large lesion.[19,22] Binding of Hup-P64A with the DNA as inferred by DNA binding experiments established the attenuated yet functional nature of P64A variant (Figure 2). Similar results indicating lower DNA binding in absence of Pro74 (corresponding to P64 in Hup) in pA104R protein (PDB ID: 6LMJ) from African swine flu virus were reported recently.[75] Undoubtedly, the DNA binding activity of Hup protein is the net sum of electrostatic interactions in the DNA binding pocket and intercalation of proline in the DNA backbone.[19,22] Indeed, replacement of proline resulted in failure of an otherwise operational pyrrolidine-mediated wedge mechanism as alanine has an aliphatic side chain instead of a ring. Previous studies evaluating the role of K62 and V63 mutations in DNA binding suggested that these residues are essential in imparting the needful flexibility for the proline mediated DNA binding.[22] Substitution of the conserved apical proline resulted in a local distortion in protein architecture as well as the failure of the intercalation mechanism. Hence, lowered DNA binding can be attributed to an equilibrium shift toward an unbound form with bipartite dependence on either the failure of the proline-dependent phosphate lock mechanism or the structural changes induced by Pro 64 in the DNA binding domain, thus underpinning the structure−function paradigm of HU protein family.

CONCLUSIONS

Overall, the study deals with delineating the role of a conserved proline at position 64 (in Hup protein) in DNA binding/clasping and structural stability. In this study, the P64A variant exhibited attenuated DNA binding, suggesting the five times weaker binding affinity. This altered functional competence can be correlated to the loss of the pyrrolidine side chain that intercalates with DNA and also to the observed differential structure−stability−dynamics features of the P64A protein. Interestingly, the P64A protein has shown enhanced local structural stability and conformational rigidity in the DNA binding region due to altered structural preferences at the β3−β4 strand. Further, P64 is also engaged in long-range contacts, and it has relayed the perturbations to the base of the saddle pocket. However, these localized perturbations and long-range effects altogether do not impart any bearing on the global stability features of the P64A protein. Conclusively, the observed attenuation in the DNA binding of P64A protein suggests the pivotal role of evolutionarily conserved proline residue in the HU family of proteins.

ASSOCIATED CONTENT

Supporting Information

The Supporting Information is available free of charge at https://pubs.acs.org/doi/10.1021/acsomega.2c01754.

Figures S1−S11 and Tables S1 and S2 supporting the data of the manuscript including a vector map and agarose gel profile, nucleotide sequencing, sodium dodecyl sulfate polyacrylamide gel electrophoresis profile showing the overexpression and purity of Hup-WT and Hup-P64A variant, three dimensional Hup structure showing the position of the Tyr residues and fluorescence spectroscopy profiles of Hup-WT and Hup-P64A, overlay of $^{1}H-^{15}N$ HSQC spectra of Hup-WT protein and Hup-P64A protein, HNCACB walk of Hup-P64A variant, fluorescence based urea denaturation experiment, MD simulation analysis of Hup-P64A, ANS binding experiment, phylogenetic analysis of HU homologues, and multiple sequence analysis of HU homologues (PDF)

Accession Codes

Hup gene UniProtKB: O25506. BMRB accession ID: 51341. Homology-modeled Hup structure at Protein Model DataBase (PMDB) with accession ID: PM0084232.

AUTHOR INFORMATION

Corresponding Author

Krishna Mohan Poluri − *Department of Biosciences and Bioengineering, Indian Institute of Technology Roorkee, Roorkee 247667 Uttarakhand, India; Centre for Nanotechnology, Indian Institute of Technology Roorkee, Roorkee 247667 Uttarakhand, India;* orcid.org/0000-0003-3801-7134; Email: krishna.poluri@bt.iitr.ac.in, mohanpmk@gmail.com

Authors

Nipanshu Agarwal − *Department of Biosciences and Bioengineering, Indian Institute of Technology Roorkee, Roorkee 247667 Uttarakhand, India;* orcid.org/0000-0001-8392-2745

Nupur Nagar − *Department of Biosciences and Bioengineering, Indian Institute of Technology Roorkee, Roorkee 247667 Uttarakhand, India*

Ritu Raj − *Centre of Biomedical Research, Lucknow 226014, India;* orcid.org/0000-0003-2788-6465

Dinesh Kumar − *Centre of Biomedical Research, Lucknow 226014, India;* orcid.org/0000-0001-8079-6739

Complete contact information is available at: https://pubs.acs.org/10.1021/acsomega.2c01754

Notes

The authors declare no competing financial interest.

ACKNOWLEDGMENTS

Authors would like to acknowledge the NMR facility and biophysical instrument facility, at the Institute instrumentation facility at IIT-Roorkee and the High Field NMR facility at the Centre for Biomedical Research (CBMR). The authors also acknowledge the support of Ms. Nancy Jaiswal and Mr. Paras Gautam for technical support. N.A. would like to thank Department of Science and Technology, India, for research fellowship under DST-INSPIRE Ph.D scheme (IF 160568). R.R. acknowledges Council of Scientific and Industrial Research (CSIR) India, for research fellowship under CSIR-JRF scheme. K.M.P and D.K. received funding from SERB-DST, Government of India, under EMR/CRG schemes (Grant Nos. EMR/2016/001756, and CRG/2018/001329) for conducting the research.

https://doi.org/10.1021/acsomega.2c01754
ACS Omega 2022, 7, 15231−15246

■ ABBREVIATIONS

HU; histone-like; Hup; histone-like (HU) protein of *Helicobacter pylori*; PCR; polymerase chain reaction; CD; circular dichroism; NAPs; nucleoid-associated-proteins; DD; dimerization domain; DBD; DNA binding domain; IPTG; isopropyl β-D-1-thiogalactopyaranose; DBP; DNA binding protein; TFs; transcription factors; IMAC; immobilized metal ion affinity chromatography; ANS; 8-anilinonaptha-lene-1-sulfonic acid; NMR; nuclear magnetic resonance; HSQC; heteronuclear single quantum spectrum; NOEs; nuclear Overhauser effects.

■ REFERENCES

(1) Stavans, J.; Oppenheim, A. DNA - protein interactions and bacterial chromosome architecture. *Phys. Biol.* **2006**, *3*, R1−R10.

(2) Dame, R. T.; Rashid, F. Z. M.; Grainger, D. C. Chromosome organization in bacteria: mechanistic insights into genome structure and function. *Nat. Rev. Genet* **2020**, *21*, 227−242.

(3) Bramhill, D.; Kornberg, A. A Model for Initiation at Origins of DNA-Replication. *Cell* **1988**, *54*, 915−918.

(4) Li, S. S.; Waters, R. Escherichia coli strains lacking protein HU are UV sensitive due to a role for HU in homologous recombination. *J. Bacteriol.* **1998**, *180*, 3750−3756.

(5) Remesh, S. G.; Verma, S. C.; Chen, J. H.; Ekman, A. A.; Larabell, C. A.; Adhya, S.; Hammel, M. Nucleoid remodeling during environmental adaptation is regulated by HU-dependent DNA bundling. *Nat. Commun.* **2020**, *11*, 1−12.

(6) Balandina, A.; Kamashev, D.; Rouviere-Yaniv, J. The bacterial histone-like protein HU specifically recognizes similar structures in all nucleic acids - DNA, RNA, and their hybrids. *J. Biol. Chem.* **2002**, *277*, 27622−27628.

(7) Tanaka, I.; Appelt, K.; Dijk, J.; White, S. W.; Wilson, K. S. 3-a Resolution Structure of a Protein with Histone-Like Properties in Prokaryotes. *Nature* **1984**, *310*, 376−381.

(8) Altukhov, D. A.; Talyzina, A. A.; Agapova, Y. K.; Vlaskina, A. V.; Korzhenevskiy, D. A.; Bocharov, E. V.; Rakitina, T. V.; Timofeev, V. I.; Popov, V. O. Enhanced conformational flexibility of the histone-like (HU) protein from Mycoplasma gallisepticum. *J. Biomol. Struct. Dyn* **2018**, *36*, 45−53.

(9) Bhowmick, T.; Ghosh, S.; Dixit, K.; Ganesan, V.; Ramagopal, U. A.; Dey, D.; Sarma, S. P.; Ramakumar, S.; Nagaraja, V. Targeting Mycobacterium tuberculosis nucleoid-associated protein HU with structure-based inhibitors. *Nat. Commun.* **2014**, *5*, 4124.

(10) Le Meur, R.; Loth, K.; Culard, F.; Castaing, B.; Landon, C. Backbone assignment of the three dimers of HU from Escherichia coli at 293 K: EcHUα 2, EcHUβ 2 and EcHUαβ. *Biomol. NMR assign.* **2015**, *9*, 359−363.

(11) Agapova, Y. K.; Altukhov, D. A.; Timofeev, V. I.; Stroylov, V. S.; Mityanov, V. S.; Korzhenevskiy, D. A.; Vlaskina, A. V.; Smirnova, E. V.; Bocharov, E. V.; Rakitina, T. V. Structure-based inhibitors targeting the alpha-helical domain of the Spiroplasma melliferum histone-like HU protein. *Sci. Rep.* **2020**, *10*, 15128.

(12) White, S. W.; Wilson, K. S.; Appelt, K.; Tanaka, I. The high-resolution structure of DNA-binding protein HU from Bacillus stearothermophilus. *Acta Crystallogr. D Biol. Crystallogr.* **1999**, *55*, 801−809.

(13) Dey, D.; Nagaraja, V.; Ramakumar, S. Structural and evolutionary analyses reveal determinants of DNA binding specificities of nucleoid-associated proteins HU and IHF. *Mol. Phylogenet. Evol.* **2017**, *107*, 356−366.

(14) Agarwal, N.; Jaiswal, N.; Gulati, K.; Gangele, K.; Nagar, N.; Kumar, D.; Poluri, K. M. Molecular Insights into Conformational Heterogeneity and Enhanced Structural Integrity of Helicobacter pylori DNA Binding Protein Hup at Low pH. *Biochemistry* **2021**, *60*, 3236−3252.

(15) Grove, A. Surface salt bridges modulate DNA wrapping by the type II DNA-binding protein TF1. *Biochemistry* **2003**, *42*, 8739−8747.

(16) Kim, D.-H.; Im, H.; Jee, J.-G.; Jang, S.-B.; Yoon, H.-J.; Kwon, A.-R.; Kang, S.-M.; Lee, B.-J. β-Arm flexibility of HU from Staphylococcus aureus dictates the DNA-binding and recognition mechanism. *Acta Crystallogr. Sect. D. Biol. Crystallogr.* **2014**, *70*, 3273−3289.

(17) Vis, H.; Mariani, M.; Vorgias, C. E.; Wilson, K. S.; Kaptein, R.; Boelens, R. Solution Structure of the HU Protein fromBacillus stearothermophilus. *J. Mol. Biol.* **1995**, *254*, 692−703.

(18) Grove, A.; Saavedra, T. C. The role of surface-exposed lysines in wrapping DNA about the bacterial histone-like protein HU. *Biochemistry* **2002**, *41*, 7597−7603.

(19) Rice, P. A.; Yang, S.; Mizuuchi, K.; Nash, H. A. Crystal structure of an IHF-DNA complex: a protein-induced DNA U-turn. *Cell* **1996**, *87*, 1295−1306.

(20) Swinger, K. K.; Lemberg, K. M.; Zhang, Y.; Rice, P. A. Flexible DNA bending in HU-DNA cocrystal structures. *EMBO J.* **2003**, *22*, 3749−3760.

(21) Lee, E. C.; Hales, L. M.; Gumport, R. I.; Gardner, J. F. The Isolation and Characterization of Mutants of the Integration Host Factor (Ihf) of Escherichia-Coli with Altered, Expanded DNA-Binding Specificities. *EMBO J.* **1992**, *11*, 305−313.

(22) Chen, C.; Ghosh, S.; Grove, A. Substrate specificity of Helicobacter pylori histone-like HU protein is determined by insufficient stabilization of DNA flexure points. *Biochem. J.* **2004**, *383*, 343−351.

(23) Sachs, G.; Weeks, D. L.; Wen, Y.; Marcus, E. A.; Scott, D. R.; Melchers, K. Acid acclimation by Helicobacter pylori. *Physiology (Bethesda)* **2005**, *20*, 429−438.

(24) Krulwich, T. A.; Sachs, G.; Padan, E. Molecular aspects of bacterial pH sensing and homeostasis. *Nat. rev. Microbiol.* **2011**, *9*, 330−343.

(25) Almarza, O.; Núñez, D.; Toledo, H. The DNA-Binding Protein HU has a Regulatory Role in the Acid Stress Response Mechanism in H elicobacter pylori. *Helicobacter* **2015**, *20*, 29−40.

(26) Álvarez, A.; Toledo, H. J. H. The histone-like protein HU has a role in gene expression during the acid adaptation response in Helicobacter pylori. *Helicobacter* **2017**, *22*, No. e12381.

(27) Dorman, C. J. Function of nucleoid-associated proteins in chromosome structuring and transcriptional regulation. *J. Mol. Microbiol. Biotechnol.* **2015**, *24*, 316−331.

(28) Kannan, A.; Camilloni, C.; Sahakyan, A. B.; Cavalli, A.; Vendruscolo, M. A Conformational Ensemble Derived Using NMR Methyl Chemical Shifts Reveals a Mechanical Clamping Transition That Gates the Binding of the HU Protein to DNA. *J. Am. Chem. Soc.* **2014**, *136*, 2204−2207.

(29) Jaiswal, N.; Agarwal, N.; Kaur, A.; Tripathi, S.; Gahlay, G. K.; Arora, A.; Mithu, V. S.; Poluri, K. M.; Kumar, D. Molecular interaction between human SUMO-I and histone like DNA binding protein of Helicobacter pylori (Hup) investigated by NMR and other biophysical tools. *Int. J. Biol. Macromol.* **2019**, *123*, 446−456.

(30) Jaiswal, N.; Raikwal, N.; Pandey, H.; Agarwal, N.; Arora, A.; Poluri, K. M.; Kumar, D. NMR elucidation of monomer-dimer transition and conformational heterogeneity in histone-like DNA binding protein of Helicobacter pylori. *Magn. Reson. Chem.* **2018**, *56*, 285−299.

(31) Gulati, K.; Gangele, K.; Kumar, D.; Poluri, K. M. An inter-switch between hydrophobic and charged amino acids generated druggable small molecule binding pocket in chemokine paralog CXCL3. *Arch. Biochem. Biophys.* **2019**, *662*, 121−128.

(32) Gulati, K.; Gangele, K.; Agarwal, N.; Jamsandekar, M.; Kumar, D.; Poluri, K. M. Molecular cloning and biophysical characterization of CXCL3 chemokine. *Int. J. Biol. Macromol.* **2018**, *107*, 575−584.

(33) Warren, J. R.; Gordon, J. A. On the refractive indices of aqueous solutions of urea. *J. Phys. Chem.* **1966**, *70*, 297−300.

(34) Chatterjee, A.; Krishna Mohan, P. M.; Prabhu, A.; Ghosh-Roy, A.; Hosur, R. V. Equilibrium unfolding of DLC8 monomer by urea and guanidine hydrochloride: Distinctive global and residue level features. *Biochimie* **2007**, *89*, 117−134.

https://doi.org/10.1021/acsomega.2c01754
ACS Omega 2022, 7, 15231−15246

(35) Mohan, P. K.; Chakraborty, S.; Hosur, R. V. Hierarchy of local structural and dynamics perturbations due to subdenaturing urea in the native state ensemble of DLC8 dimer. *Biophys. Chem.* **2010**, *153*, 17−26.
(36) Raj, R.; Agarwal, N.; Raghavan, S.; Chakraborti, T.; Poluri, K. M.; Kumar, D. Exquisite binding interaction of 18β-Glycyrrhetinic acid with histone like DNA binding protein of Helicobacter pylori: A computational and experimental study. *Int. J. Biol. Macromol.* **2020**, *161*, 231−246.
(37) Joshi, N.; Kumar, D.; Poluri, K. M. Elucidating the Molecular Interactions of Chemokine CCL2 Orthologs with Flavonoid Baicalin. *ACS Omega* **2020**, *5*, 22637−22651.
(38) Baxter, N. J.; Williamson, M. P. Temperature dependence of 1 H chemical shifts in proteins. *J. Biomol. NMR* **1997**, *9*, 359−369.
(39) Sharma, M.; Kumar, D.; Poluri, K. M. Elucidating the pH-Dependent Structural Transition of T7 Bacteriophage Endolysin. *Biochemistry* **2016**, *55*, 4614−4625.
(40) Farrow, N. A.; Muhandiram, R.; Singer, A. U.; Pascal, S. M.; Kay, C. M.; Gish, G.; Shoelson, S. E.; Pawson, T.; Forman-Kay, J. D.; Kay, L. E. Backbone dynamics of a free and phosphopeptide-complexed Src homology 2 domain studied by 15N NMR relaxation. *Biochemistry* **1994**, *33*, 5984−6003.
(41) Abraham, M. J.; Murtola, T.; Schulz, R.; Páll, S.; Smith, J. C.; Hess, B.; Lindahl, E. GROMACS: High performance molecular simulations through multi-level parallelism from laptops to supercomputers. *SoftwareX* **2015**, *1*, 19−25.
(42) Jorgensen, W. L.; Chandrasekhar, J.; Madura, J. D.; Impey, R. W.; Klein, M. L. Comparison of Simple Potential Functions for Simulating Liquid Water. *J. Chem. Phys.* **1983**, *79*, 926−935.
(43) Lindorff-Larsen, K.; Piana, S.; Palmo, K.; Maragakis, P.; Klepeis, J. L.; Dror, R. O.; Shaw, D. E. Improved side-chain torsion potentials for the Amber ff99SB protein force field. *Proteins* **2010**, *78*, 1950−1958.
(44) Dalal, V.; Kumar, P.; Rakhaminov, G.; Qamar, A.; Fan, X.; Hunter, H.; Tomar, S.; Golemi-Kotra, D.; Kumar, P. Repurposing an ancient protein core structure: Structural studies on FmtA, a novel esterase of Staphylococcus aureus. *J. Mol. Biol.* **2019**, *431*, 3107−3123.
(45) Raj, R.; Agarwal, N.; Raghavan, S.; Chakraborti, T.; Poluri, K. M.; Pande, G.; Kumar, D. Epigallocatechin Gallate with Potent Anti-Helicobacter pylori Activity Binds Efficiently to Its Histone-like DNA Binding Protein. *ACS Omega* **2021**, *6*, 3548−3570.
(46) Kumar, S.; Stecher, G.; Li, M.; Knyaz, C.; Tamura, K. MEGA X: Molecular Evolutionary Genetics Analysis across Computing Platforms. *Mol. Biol. Evol.* **2018**, *35*, 1547−1549.
(47) Letunic, I.; Bork, P. Interactive Tree Of Life (iTOL): an online tool for phylogenetic tree display and annotation. *Bioinformatics* **2007**, *23*, 127−128.
(48) Schneider, T. D.; Stephens, R. M. Sequence logos: a new way to display consensus sequences. *Nucleic Acids Res.* **1990**, *18*, 6097−6100.
(49) Balandina, A.; Kamashev, D.; Rouviere-Yaniv, J. The bacterial histone-like protein HU specifically recognizes similar structures in all nucleic acids: DNA, RNA, and their hybrids. *J. Biol. Chem.* **2002**, *277*, 27622−27628.
(50) Krylov, A. S.; Zasedateleva, O. A.; Prokopenko, D. V.; Rouviere-Yaniv, J.; Mirzabekov, A. D. Massive parallel analysis of the binding specificity of histone-like protein HU to single-and double-stranded DNA with generic oligodeoxyribonucleotide microchips. *Nucleic Acids Res.* **2001**, *29*, 2654−2660.
(51) Dorman, C. J. Function of nucleoid-associated proteins in chromosome structuring and transcriptional regulation. *Microb. Physiol.* **2015**, *24*, 316−331.
(52) Deng, X.; Walker, R. G.; Morris, J.; Davidson, W. S.; Thompson, T. B. Role of Conserved Proline Residues in Human Apolipoprotein A-IV Structure and Function. *J. Biol. Chem.* **2015**, *290*, 10689−10702.
(53) Yutani, K.; Hayashi, S.; Sugisaki, Y.; Ogasahara, K. Role of conserved proline residues in stabilizing tryptophan synthase α subunit: analysis by mutants with alanine or glycine. *Proteins: Struct. Funct. Bioinform.* **1991**, *9*, 90−98.
(54) Cierpicki, T.; Otlewski, J. Amide proton temperature coefficients as hydrogen bond indicators in proteins. *J. Biomol. NMR* **2001**, *21*, 249−261.
(55) Cierpicki, T.; Zhukov, I.; Byrd, R. A.; Otlewski, J. Hydrogen bonds in human ubiquitin reflected in temperature coefficients of amide protons. *J. Magn. Reson.* **2002**, *157*, 178−180.
(56) Krishna Mohan, P. M.; Hosur, R. V. NMR insights into dynamics regulated target binding of DLC8 dimer. *Biochem. Biophys. Res. Commun.* **2007**, *355*, 950−955.
(57) Krishna Mohan, P.; Hosur, R. V. Structure-function-folding relationships and native energy landscape of dynein light chain protein: nuclear magnetic resonance insights. *J. Biosci. (Bangalore)* **2009**, *34*, 465−479.
(58) Huilgol, D.; Venkataramani, P.; Nandi, S.; Bhattacharjee, S. Transcription Factors That Govern Development and Disease: An Achilles Heel in Cancer. *Genes* **2019**, *10*, 794.
(59) Borca, M. V.; Irusta, P. M.; Kutish, G. F.; Carrillo, C.; Afonso, C. L.; Burrage, A. T.; Neilan, J. G.; Rock, D. L. A structural DNA binding protein of African swine fever virus with similarity to bacterial histone-like proteins. *Arch. Virol.* **1996**, *141*, 301−313.
(60) Kobayashi, T.; Takahara, M.; Miyagishima, S. Y.; Kuroiwa, H.; Sasaki, N.; Ohta, N.; Matsuzaki, M.; Kuroiwa, T. Detection and localization of a chloroplast-encoded HU-like protein that organizes chloroplast nucleoids. *Plant Cell* **2002**, *14*, 1579−1589.
(61) White, M. F.; Bell, S. D. Holding it together: chromatin in the Archaea. *Trends Genet.* **2002**, *18*, 621−626.
(62) Kurahashi, R.; Tanaka, S. I.; Takano, K. Activity-stability trade-off in random mutant proteins. *J. Biosci. Bioeng.* **2019**, *128*, 405−409.
(63) Vainauskas, S.; Menon, A. K. A conserved proline in the last transmembrane segment of Gaa1 is required for glycosylphosphatidylinositol (GPI) recognition by GPI transamidase. *J. Biol. Chem.* **2004**, *279*, 6540−6545.
(64) Joseph, P. R. B.; Poluri, K. M.; Gangavarapu, P.; Rajagopalan, L.; Raghuwanshi, S.; Richardson, R. M.; Garofalo, R. P.; Rajarathnam, K. Proline substitution of dimer interface β-strand residues as a strategy for the design of functional monomeric proteins. *Biophys. J.* **2013**, *105*, 1491−1501.
(65) Charbonnier, J. B.; Belin, P.; Moutiez, M.; Stura, E. A.; Quemeneur, E. On the role of the cis-proline residue in the active site of DsbA. *Protein Sci.* **1999**, *8*, 96−105.
(66) Davis, J. E.; Alghanmi, A.; Gundampati, R. K.; Jayanthi, S.; Fields, E.; Armstrong, M.; Weidling, V.; Shah, V.; Agrawal, S.; Koppolu, B. P.; Zaharoff, D. A.; Kumar, T. K. S. Probing the role of proline-135 on the structure, stability, and cell proliferation activity of human acidic fibroblast growth factor. *Arch. Biochem. Biophys.* **2018**, *654*, 115−125.
(67) Singh, M. K.; Manoj, N. Structural role of a conserved active site cis proline in the T hermotoga maritima acetyl esterase from the carbohydrate esterase family 7. *Proteins: Struct. Funct. Bioinform.* **2017**, *85*, 694−708.
(68) Reidhaar-Olson, J. F.; Parsell, D. A.; Sauer, R. T. An essential proline in. lambda. repressor is required for resistance to intracellular proteolysis. *Biochemistry* **1990**, *29*, 7563−7571.
(69) Jaakkola, P.; Mole, D. R.; Tian, Y.-M.; Wilson, M. I.; Gielbert, J.; Gaskell, S. J.; Kriegsheim, A. v.; Hebestreit, H. F.; Mukherji, M.; Schofield, C. J.; et al. Targeting of HIF-α to the von Hippel-Lindau ubiquitylation complex by O2-regulated prolyl hydroxylation. *Science* **2001**, *292*, 468−472.
(70) Sidorkina, O. M.; Laval, J. Role of the N-terminal proline residue in the catalytic activities of the Escherichia coli Fpg protein. *J. Biol. Chem.* **2000**, *275*, 9924−9929.
(71) Baig, I. A.; Gedi, V.; Lee, S. C.; Koh, S. H.; Yoon, M. Y. Role of a highly conserved proline-126 in ThDP binding of Mycobacterium tuberculosis acetohydroxyacid synthase. *Enzyme Microb. Technol.* **2013**, *53*, 243−249.
(72) Spencer, J. V.; Arndt, K. M. A TATA binding protein mutant with increased affinity for DNA directs transcription from a reversed TATA sequence in vivo. *Mol. Cell. Biol.* **2002**, *22*, 8744−8755.

https://doi.org/10.1021/acsomega.2c01754
ACS Omega 2022, 7, 15231−15246

(73) Khadake, J. R.; Rao, M. R. Condensation of DNA and chromatin by an SPKK-containing octapeptide repeat motif present in the C-terminus of histone H1. *Biochemistry* **1997**, *36*, 1041−1051.
(74) Bharath, M. M. S.; Ramesh, S.; Chandra, N. R.; Rao, M. R. S. Identification of a 34 amino acid stretch within the C-terminus of histone H1 as the DNA-condensing domain by site-directed mutagenesis. *Biochemistry* **2002**, *41*, 7617−7627.
(75) Frouco, G.; Freitas, F. B.; Coelho, J.; Leitao, A.; Martins, C.; Ferreira, F. DNA-Binding Properties of African Swine Fever Virus pA104R, a Histone-Like Protein Involved in Viral Replication and Transcription. *J. Virol.* **2017**, *91*, e02498.

https://doi.org/10.1021/acsomega.2c01754
ACS Omega 2022, 7, 15231−15246